Modern Pathology (2014) 27, 1116–1125
© 2014 USCAP, Inc All rights reserved 0893-3952/14 $32.00

Inhibition of *ZEB1* by miR-200 characterizes *Helicobacter pylori*-positive gastric diffuse large B-cell lymphoma with a less aggressive behavior

Wei-Ting Huang[1], Sung-Hsin Kuo[2], Ann-Lii Cheng[2] and Chung-Wu Lin[1]

[1]*Department of Pathology, National Taiwan University Hospital of Medicine, Taipei, Taiwan and* [2]*Department of Oncology, National Taiwan University Hospital, Taipei, Taiwan*

Primary gastric diffuse large B-cell lymphomas may or may not have a concurrent component of mucosa-associated lymphoid tissue lymphoma. Diffuse large B-cell lymphoma/mucosa-associated lymphoid tissue lymphomas are often associated with *Helicobacter pylori* (*H. pylori*) infection, suggesting that the large cells are transformed from mucosa-associated lymphoid tissue lymphomas. In contrast, only limited data are available on the clinical and molecular features of pure gastric diffuse large B-cell lymphomas. In 102 pure gastric diffuse large B-cell lymphomas, we found *H. pylori* infection in 53% of the cases. *H. pylori*-positive gastric diffuse large B-cell lymphomas were more likely to present at an earlier stage (73% *vs* 52% at stage I/II, $P=0.03$), to achieve complete remission (75% *vs* 43%, $P=0.001$), and had a better 5-year disease-free survival rate (73% *vs* 29%, $P<0.001$) than *H. pylori*-negative gastric diffuse large B-cell lymphomas. Through genome-wide expression profiles of both miRNAs and mRNAs in nine *H. pylori*-positive and nine *H. pylori*-negative gastric diffuse large B-cell lymphomas, we identified inhibition of *ZEB1* (zinc-finger E-box-binding homeobox 1) by miR-200 in *H. pylori*-positive gastric diffuse large B-cell lymphomas. *ZEB1*, a transcription factor for marginal zone B cells, can suppress *BCL6*, the master transcription factor for germinal center B cells. In 30 *H. pylori*-positive and 30 *H. pylori*-negative gastric diffuse large B-cell lymphomas, we confirmed that *H. pylori*-positive gastric diffuse large B-cell lymphomas had higher levels of miR-200 by qRT-PCR, and lower levels of *ZEB1* and higher levels of *BCL6* using immunohistochemistry. As *BCL6* is a known predictor of a better prognosis in gastric diffuse large B-cell lymphomas, our data demonstrate that inhibition of *ZEB1* by miR-200, with secondary increase in *BCL6*, is a molecular event that characterizes *H. pylori*-positive gastric diffuse large B-cell lymphomas with a less aggressive behavior.
Modern Pathology (2014) **27,** 1116–1125; doi:10.1038/modpathol.2013.229; published online 3 January 2014

Keywords: gastric diffuse large B-cell lymphoma; miR-200; *ZEB1*

Most primary non-Hodgkin lymphomas of the stomach can be classified into the indolent mucosa-associated-lymphoid-tissue lymphomas derived from marginal zone B cells and the aggressive diffuse large B-cell lymphomas.[1]

In 20% of gastric diffuse large B-cell lymphomas, a concurrent component of mucosa-associated-lymphoid-tissue lymphoma can be identified. About 65% of these diffuse large B-cell lymphoma/mucosa-associated-lymphoid-tissue lymphomas are associated with *Helicobacter pylori* (*H. pylori*) infection and can be cured by *H. pylori* eradication therapy. These clinical features of diffuse large B-cell lymphoma/mucosa-associated-lymphoid-tissue lymphomas are similar to those of mucosa-associated-lymphoid-tissue lymphomas, suggesting a common marginal zone B-cell origin with mucosa-associated-lymphoid-tissue lymphomas, and that the large cells are transformed from the mucosa-associated-lymphoid-tissue lymphomas.[2,3]

In contrast, most gastric diffuse large B-cell lymphomas do not have a component of mucosa-associated-lymphoid-tissue lymphoma. Data on the clinical behavior, the cellular origin, and molecular features of these diffuse large B-cell lymphomas are still limited. Among these diffuse large B-cell lymphoma diffuse large B-cell lymphomas, the incidence of *H. pylori* infection varies from 15 to 50%.[2,3] Although higher expression of *BCL6*, the

Correspondence: Dr C-W Lin, MD, PhD, Department of Pathology, National Taiwan University College of Medicine, 1-1, Jen-Ai Road, Taipei 100, Taiwan.
E-mail: chungwulin@yahoo.com
Received 11 August 2013; revised 21 October 2013; accepted 21 October 2013; published online 3 January 2014

master transcription factor for the formation of germinal center B cells, is a predictor of a better prognosis in gastric diffuse large B-cell lymphomas,[4] it is unclear how *H. pylori* infection may affect directly this molecular event and secondarily the clinical manifestations.

Epithelial–mesenchymal transition is a process occurring during embryonic development. Through epithelial–mesenchymal transition, epithelial cells lose polarity and intercellular contact, and become mesenchyme-like with an increased migratory ability.[5] *ZEB1* (zinc-finger E-box-binding homeobox 1), which is regulated by miR-200, is a transcription factor for the induction of epithelial–mesenchymal transition in epithelial cells. The process of epithelial–mesenchymal transition is also found in cancer cells of the epithelial origin. Increased expression of *ZEB1* or decreased expression of miR-200 is associated with epithelial–mesenchymal transition and metastasis of cancer cells.[6,7]

Although studies on *ZEB1* focus mostly on its roles in epithelial–mesenchymal transition and metastasis, it is becoming evident that *ZEB1* is also critical in the development of hematopoietic cells, including both B cells and T cells. For the B-lineage, *ZEB1* may inhibit *BCL6*, the master transcription factor for the formation of germinal center B cells,[8] and is required for the normal development of marginal zone B cells and the production of immunoglobulin M.[9,10] Consistent with these data, overexpression of *ZEB1* induces a more aggressive behavior of diffuse large B-cell lymphoma of the lymph nodes.[11] For the T-lineage, *ZEB1* regulates T-cell development.[12–14] Loss of *ZEB1* in knockout mice accelerates the development of adult T-cell leukemia.[15]

In this study, we found that *H. pylori*-positive gastric diffuse large B-cell lymphomas had less lymph node metastasis and a better response to chemotherapy. Genome-wide expression profiles of both miRNAs and mRNAs identified inhibition of *ZEB1* by miR-200, with secondary induction of *BCL6*, as one of the molecular events that characterized *H. pylori*-positive gastric diffuse large B-cell lymphomas, and partially accounted for the less aggressive behavior of *H. pylori*-positive gastric diffuse large B-cell lymphomas.

Materials and methods

Tissue Samples

From the archives at the Pathology Department of the National Taiwan University Hospital, cases with a diagnosis of gastric diffuse large B-cell lymphoma after 2000 were selected. Cases with incomplete induction therapy, with additional *H. pylori* eradication therapy, or with a component of mucosa-associated-lymphoid-tissue lymphoma at the time of diagnosis or during follow-up were excluded. A total of 102 cases were finally selected. The ethics committee of the National Taiwan University Hospital approved this study. The diagnosis of diffuse large B-cell lymphoma was based on the WHO criteria, characterized by diffuse infiltrates of large lymphoid cells, without a detectible component of mucosa-associated-lymphoid-tissue lymphoma. All the specimens were first examined on serial H&E sections. A case with dense clusters of curved spiral bacilli was declared *H pylori*-positive. A Diff-Quik stain and a slide urease test were performed if the results of H&E stains were equivocal or negative. Clinical staging was performed with endoscopic ultrasonography, abdominal CT, or MRI. Stage-I_E diffuse large B-cell lymphomas were limited to the stomach. Stage-II_{E1} diffuse large B-cell lymphomas involved both the stomach and peri-gastric lymph nodes. Stage-II_{E2} diffuse large B-cell lymphomas involved both the stomach and more distant abdominal lymph nodes, such as mesenteric and para-aortic lymph nodes. Stage-III_E diffuse large B-cell lymphomas involved extra-abdominal lymph nodes. Stage-IV_E diffuse large B-cell lymphomas involved the bone marrow. Clinical data, treatments, and outcomes were extracted from the medical records.

Genome-Wide miRNA Profiles in 18 Gastric Diffuse Large B-cell Lymphomas

A series of 18 gastric diffuse large B-cell lymphomas including nine *H. pylori*-positive and nine *H. pylori*-negative gastric diffuse large B-cell lymphomas were used. The nCounter miRNA Expression Analysis System (NanoString Technologies, Seattle, WA, USA) was used to obtain the expression profiles of 633 human miRNAs.[16–18] A panel of six synthetic miRNAs was used as internal positive controls. Approximately 0.1 μg of total RNAs were extracted from formalin-fixed paraffin-embedded tissue blocks. Mature miRNAs were ligated to sequence-specific miRtags, and the miRtagged-mature miRNAs were hybridized to fluorescent reporter probes and to capture probes. After hybridization, the samples were immobilized to a solid-phase cartridge, and a CCD digital analyzer was used for data acquisition. The data were normalized to the internal positive controls. The normalized data were submitted as Supplementary Table S1.

Genome-Wide mRNA Expression Profiles in 18 Gastric Diffuse Large B-cell Lymphomas

The Agilent SurePrint G3 Human GE 8×60 K Microarrays were used according to the manufacturer's recommendations (Agilent Technologies, Santa Clara, CA, USA). Approximately 0.2 μg of total RNAs were reverse-transcribed, amplified, and Cy3-labeled with a Low Input Quick-Amp Labeling kit. The Cy3-labeled cRNAs were fragmented to an average size of 50–100 nucleotides and hybridized to the microarrays at 65 °C for 40 h. After washing, the microarrays were scanned with an Agilent

microarray scanner at 535 nm for Cy3. The scanned images were analyzed with the Feature Extraction 10.5.1.1 software. The normalized data are submitted in Supplementary Table S2.

Bioinformatics

Two-sample comparisons between nine *H. pylori*-positive and nine *H. pylori*-negative gastric diffuse large B-cell lymphomas were performed. Hierarchical clustering was performed with the Genesis software.[19]

Quantitative RT-PCR for miRNA-200

Total RNAs were extracted from formalin-fixed, paraffin-embedded tissue blocks with the Trizol method. A stem-loop RT-PCR for miRNAs was performed according to a published protocol with modification.[20,21]

For RT, the reverse primers were: 5′-N44-ACA TCG-3′ for miR-200a, 5′-N44-TCATCA-3′ for miR-200b, and 5′-N44-TCCATC-3′ for miR-200c, where N44 is 5′-GTCGTATCCATGGCAGGGTCCGAGGTAT TCGCCATGGATACGAC-3′. The RT mixture included 0.1 μM miRNA-specific stem–loop RT primer, 10 mM dNTPs, 50 mM Tris-HCl at pH 8.3, 75 mM KCl, 3 mM $MgCl_2$, 0.1 M DTT, 100 units of reverse transcriptase, and 1 μg RNA in a final volume of 20 μl. The mixture was incubated at 42 °C for 80 min.

For PCR, an universal reverse PCR primer, 5′-TGGCAGGGTCCGAGGT-3′, and miRNA-specific forward primers were used. The specific forward primers were: 5′-GGGTAACACTGTCTGGTAA-3′ for miR-200a, 5′-GGGTAATACTGCCTGGTAA-3′ for miR-200b, and 5′-GGGTAATACTGCCGGGTAAT-3′ for miR-200 c. Real-time PCRs were carried out in a 20-μl reaction mixture that included 5 μl diluted cDNA, 0.1 μM miRNA-specific forward primer, 0.1 μM universal reverse primer, and 10 μl of SYBR Green PCR master mix (TOYOBO, Tokyo, Japan). A PCR cycle consisted of denaturation at 95 °C for 15 s and annealing at 60 °C for 1 min. The PCR products, 54 ~ 58 bp for miRNAs and 140 bp for U6, were confirmed by 8% acrylamide gel and sequencing. The difference between the threshold cycles of a specific miRNA and U6 snRNA, dC_t (C_{tmiRNA}–C_{tU6}), was calculated from the mean values of duplicate measurements. This definition of dC_t implies an inverse correlation between dC_ts and miRNA levels.

Immunohistochemistry for *ZEB1* and *BCL6*

Immunoperoxidase stains on formalin-fixed, paraffin-embedded tissue sections with a *ZEB1* antibody (1:100, rabbit polyclonal, Novus, Littleton, CO, USA) and a *BCL6* antibody (1:100, PG-B6P, mouse monoclonal, Abcam, Cambridge, MA, USA). Antigen retrieval was performed in Tris buffer at pH 6 for *ZEB1* and at pH8 for *BCL6*. The primary antibody was applied to the slides at 37 °C for 45 min. Biotin-conjugated secondary antibodies, peroxidase-conjugated streptavidin, and DAB were used sequentially for completing the reactions. The percentages of positive cells, as averages of 10 randomly selected high-power fields, were determined.

Table 1 Clinical features of *H. pylori*-positive and *H. pylori*-negative gastric diffuse large B-cell lymphomas

	Total (%)	*H. pylori-positive (%)*	*H. pylori-negative (%)*	P
Total no.	102 (100)	48 (47)	54 (53)	
Sex				
Female	55 (54)	24 (50)	31 (57)	0.454
Male	47 (46)	24 (50)	23 (43)	
Age (years)				
<60	47 (48)	22 (46)	25 (46)	0.963
≥60	55 (52)	26 (54)	29 (54)	
Stage				
I–II	63 (62)	35 (73)	28 (52)	0.029
III/IV	39 (38)	13 (27)	26 (48)	
ECOG				
0–1	87 (85)	45 (94)	42 (78)	0.023
≥2	15 (15)	3 (6)	12 (22)	
LDH				
Normal	56 (55)	33 (69)	23 (43)	0.008
High	46 (45)	15 (31)	31 (57)	
IPI risk group				
0–1	54 (53)	32 (67)	22 (41)	0.009
≥2	48 (47)	16 (33)	32 (59)	
Chemotherapy response				
CR	59 (58)	36 (75)	23 (43)	0.001
PR + SD + PD	43 (42)	12 (25)	31 (57)	
Chemotherapy regimens				
CHOP or CEOP	60 (59)	25 (52)	35 (65)	0.304
Rituximab-based[a]	25 (24)	15 (31)	10 (18)	
Others[b]	17 (17)	8 (17)	9 (17)	
5-Y EFS[c]	46.7%	72.7%	29.1%	<0.001
5-Y OS[c]	51.1%	73.6%	35.4%	<0.001

Abbreviations: CHOP, (cyclophosphamide, doxorubicin, vincristine, prednisolone); CEOP (cyclophosphamide, epirubicin, vincristine, prednisolone); CR, complete remission; ECOG, Eastern Cooperative Oncology Group; EFS, event-free survival; *H. pylori*, *Helicobacter pylori*; IPI, International Prognostic Index; PR, partial remission; SD, stable disease; PD, progression; OS, overall survival.
[a]Rituximab-CHOP, Rituximab-CEOP, Rituximab-COP.
[b]Others: CNOP (cyclophosphamide, mitoxantrone, vincristine, prednisolone), COP (cyclophosphamide, vincristine, prednisolone), ACE (doxorubicin, cyclophosphamide, etoposide), or PACE (prednisolone-ACE).
[c]Survival was estimated by the Kaplan–Meier method and compared by log-rank test.

Results

H. pylori-Positive Gastric Diffuse Large B-cell Lymphomas have Less Lymph Node Metastasis and a Better Response to Chemotherapy than *H. pylori*-Negative Gastric Diffuse Large B-cell Lymphomas

A series of 102 gastric diffuse large B-cell lymphomas without a concurrent component of mucosa-

associated-lymphoid-tissue lymphoma was used to investigate the differences in the clinical manifestations between 48 *H. pylori*-positive and 54 *H. pylori*-negative groups (Table 1).

Table 2 miRNAs differentially expressed between *H. pylori*-negative and *H. pylori*-positive gastric diffuse large B-cell lymphomas

	P-*value*	*H. pylori*-*negative*	*H. pylori*-*positive*	*Ratio*
miR-200a	0.004	156	463	2.96
miR-200c	0.014	55	140	2.55
miR-200b	0.016	56	166	2.95
miR-520e	0.023	19	30	1.57
miR-507	0.042	27	13	0.46
miR-544	0.046	71	1821	25.47
miR-142-3p	0.049	3312	614	0.19
miR-513b	0.050	18	8	0.46

Out of 633 miRNAs, eight are differentially expressed between *H. pylori*-negative and *H. pylori*-positive gastric diffuse large B-cell lymphomas. They are listed according to the *P*-values.
The columns are: name of miRNA, *P*-value, average level in *H. pylori*-negative gastric diffuse large B-cell lymphomas, average level in *H. pylori*-positive gastric diffuse large B-cell lymphomas, and ratio of the average level in *H. pylori*-positive gastric diffuse large B-cell lymphomas to the average level in *H. pylori*-negative gastric diffuse large B-cell lymphomas.

Regardless of the *H. pylori* status, gastric diffuse large B-cell lymphomas do not show a gender bias. At the time of presentation, the patients have a median age of about 60 years. However, the *H. pylori*-positive group is more likely to present at an early stage than the *H. pylori*-negative group (73% *vs* 52% at stage I/II, $P=0.03$). Consistent with the earlier staging, the *H. pylori*-positive group has a better Eastern Cooperative Oncology Group (ECOG) performance status ($P=0.023$), is more likely to have a normal LDH level ($P=0.008$), and belongs to a lower International Prognostic Index (IPI) risk group ($P=0.009$).

The *H. pylori*-positive and *H. pylori*-negative groups received similar chemotherapy regimens. Significantly, 75% of the *H. pylori*-positive group but only 43% of the *H. pylori*-negative group achieved complete remission ($P=0.001$). Consistent with the better complete remission rate, the *H. pylori*-positive group had a higher 5-year event-free survival rate (73% *vs* 29%, $P<0.001$) and a higher 5-year overall survival rate (74% *vs* 35%, $P<0.001$) than the *H. pylori*-negative group. Note that the outcome parameters were all better in the *H. pylori*-positive group than in the *H. pylori*-negative group by a margin of at least 30%, which cannot be totally

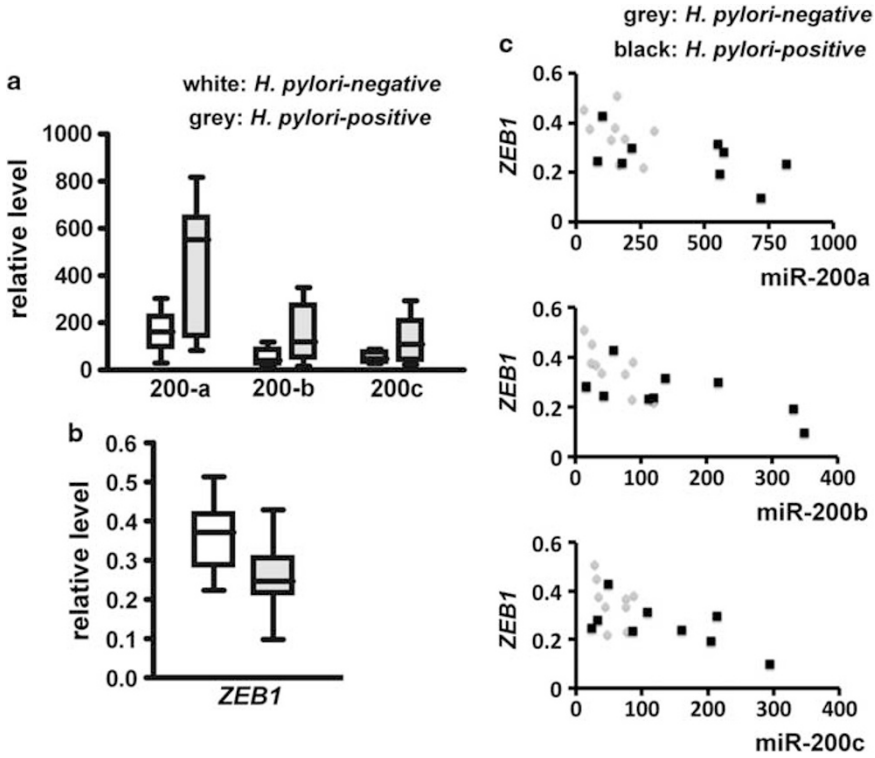

Figure 1 Inhibition of *ZEB1* by miRNA-200 characterized *H. pylori*-positive gastric diffuse large B-cell lymphomas. (**a**) *H. pylori*-positive gastric diffuse large B-cell lymphomas have higher levels of miR-200 a, b, and c. *y* axis: miR-200 expression levels measured by the NanoString technology; *x* axis: miR-200, a, b, or c in nine HP-negative (white) or nine HP-positive (gray) gastric diffuse large B-cell lymphomas. (**b**) *H. pylori*-positive gastric diffuse large B-cell lymphomas have lower levels of *ZEB1*. *y* axis: *ZEB1* expression levels measured by microarrays; *x* axis: *ZEB1* in nine *H. pylori*-negative (white) or nine *H. pylori*-positive (gray) gastric diffuse large B-cell lymphomas. (**c**) Inverse correlations between *ZEB1* and miR-200 in gastric diffuse large B-cell lymphomas. *y* axis: *ZEB1* levels; *x* axis: miR-200 a, b, or c. Gray: nine *H. pylori*-negative gastric diffuse large B-cell lymphomas; black: nine *H. pylori*-positive gastric diffuse large B-cell lymphomas. Correlation coefficients at -0.60 at $P=0.008$ for miR-200a, -0.71 at $P<0.001$ for miR-200b, and -0.63 at $P=0.005$ for miR-200c, respectively.

Table 3 mRNAs differentially expressed between *H. pylori*-negative and *H. pylori*-positive gastric diffuse large B-cell lymphomas

Gene	P	*HP−*	*HP+*			*Target*
CYFIP2	0.010	0.33	0.25	0.75	Cytoplasmic *FMR1*-interacting protein 2	miR-544
GATAD2A	0.011	0.44	0.32	0.72	*GATA* zinc-finger domain containing 2A	No
PHPT1	0.014	0.43	0.54	1.25	Phosphohistidine phosphatase 1	No
HCRT	0.017	0.43	0.29	0.68	Hypocretin (orexin) neuropeptide precursor	No
KRT18	0.019	0.14	0.22	1.60	Keratin 18	No
SDHA	0.024	0.07	0.14	2.02	Succinate dehydrogenase complex, subunit A	No
FUBP3	0.024	0.29	0.22	0.76	Far upstream element (FUSE)-binding protein 3	miR-200
ZEB1	0.025	0.37	0.26	0.70	Zinc-finger E-box-binding homeobox 1	miR-200
WDR13	0.026	0.16	0.20	1.28	WD repeat domain 13	No
SOCS1	0.029	0.80	0.59	0.74	Suppressor of cytokine signaling 1	No
ANXA13	0.031	0.13	0.08	0.62	Annexin A13	No
CCDC69	0.032	0.17	0.12	0.72	Coiled-coil domain containing 69	No
DAXX	0.033	0.28	0.23	0.83	Death-domain-associated protein	No
OR10A2	0.034	0.13	0.09	0.69	Olfactory receptor, family 10A, member 2	No
FAM113A	0.038	0.22	0.16	0.70	Family with sequence similarity 113, member A	No
CACNG6	0.038	0.13	0.08	0.66	Calcium channel, voltage-dependent, γ subunit 6	No
PCMT1	0.040	0.64	0.55	0.86	Protein-L-isoaspartate O-methyltransferase	No
TMEM52	0.040	0.07	0.15	2.13	Transmembrane protein 52	No
AAK1	0.042	1.05	0.88	0.84	*AP2*-associated kinase 1	No
MARK4	0.043	0.32	0.24	0.75	*MAP*/microtubule affinity-regulating kinase 4	No
SNX15	0.044	0.22	0.16	0.75	Sorting nexin 15	No
WDR12	0.044	0.17	0.12	0.75	WD repeat domain 12	No
TMEM54	0.045	0.17	0.29	1.78	Transmembrane protein 54	No
ATN1	0.046	0.17	0.21	1.25	Atrophin 1	No
GLTSCR1	0.048	0.37	0.28	0.77	Glioma tumor suppressor candidate region gene 1	No
PRR11	0.048	0.28	0.21	0.74	Proline-rich 11	No
CIDEB	0.049	0.18	0.14	0.79	Cell death-inducing *DFFA*-like effector b	No
SNX4	0.049	0.23	0.15	0.65	Sorting nexin 4	No
SHBG	0.049	0.14	0.09	0.66	Sex hormone-binding globulin	No
PSCA	0.050	0.06	0.28	4.39	Prostate stem cell antigen	No

Out of 42 405 probes, 30 mRNAs with differential expressions between *H. pylori*-negative and *H. pylori*-positive gastric diffuse large B-cell lymphomas were identified. They are listed according to the *P*-values. Noncoding genes, or genes with expression levels below 0.1, were excluded.
The columns are: gene symbol, *P*-value, average level in *H. pylori*-negative gastric diffuse large B-cell lymphomas, average level in *H. pylori*-positive gastric diffuse large B-cell lymphomas, ratio of the average level in the *H. pylori*-positive group to that in the *H. pylori*-negative group, and predicted targets identified by the miR.org program.

attributed to the 13% difference in the percentages of patients treated with Rituximab therapy (31% in the *H. pylori*-positive group *vs* 18% in the *H. pylori*-negative group).

To summarize the clinical comparisons, we found that *H. pylori*-positive gastric diffuse large B-cell lymphomas have less lymph node metastasis and a better response to chemotherapy than *H. pylori*-negative gastric diffuse large B-cell lymphomas. *H. pylori*-positive gastric diffuse large B-cell lymphoma is, therefore, a less aggressive lymphoma than *H. pylori*-negative gastric diffuse large B-cell lymphoma.

H. pylori-Positive Gastric Diffuse Large B-cell Lymphomas have Higher Levels of miR-200 than *H. pylori*-Negative Gastric Diffuse Large B-cell Lymphomas

To identify a molecular mechanism underlying the less aggressive behavior of *H. pylori*-positive gastric diffuse large B-cell lymphomas, we obtained genome-wide miRNA expression profiles in nine *H. pylori*-positive and nine *H. pylori*-negative gastric diffuse large B-cell lymphomas. This series is independent of the clinical series of 102 cases.

Out of 633 miRNAs, eight miRNAs have a difference in the expression levels between *H. pylori*-positive and *H. pylori*-negative groups (Table 2). Most significantly, miR-200a, miR-200b, and miR-200c are the three miRNAs with the most significant differential expressions (Table 2; Figure 1a). The levels for miR-200 a, b, or c are all increased by 2.5- to 3-fold in the *H. pylori*-positive group at a *P*-value <0.01.

H. pylori-Positive Gastric Diffuse Large B-cell Lymphomas have Lower Levels of *ZEB1* than *H. pylori*-Negative Gastric Diffuse Large B-cell Lymphomas

We also obtained genome-wide mRNA expression profiles in nine *H. pylori*-positive and nine *H. pylori*-negative gastric diffuse large B-cell lymphomas.

Out of 42 405 probes, 30 mRNAs were found to have different expression levels between *H. pylori*-positive and *H. pylori*-negative groups (Table 3). Owing to our interests in identifying a miRNA-mediated mechanism that distinguishes *H. pylori*-positive from *H. pylori*-negative gastric diffuse large B-cell lymphomas, we used the miR.org program to identify potential miR-200 targets out of the list of

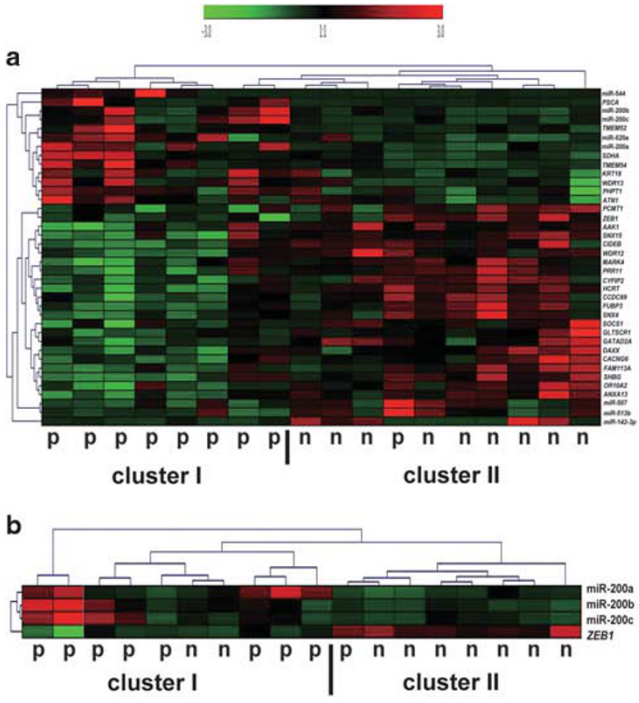

Figure 2 Hierarchical clustering of nine *H. pylori*-positive and nine *H. pylori*-negative gastric diffuse large B-cell lymphomas. (**a**) Hierarchical clustering with the whole panel of eight miRNAs and 30 mRNAs generated cluster I with eight *H. pylori*-positive gastric diffuse large B-cell lymphomas, and cluster II with nine *H. pylori*-negative gastric diffuse large B-cell lymphomas plus one *H. pylori*-positive gastric diffuse large B-cell lymphomas (8:0 *vs* 1:9, $P<0.001$). (**b**) Hierarchical clustering with miR-200 and *ZEB1* generated cluster I with eight *H. pylori*-positive gastric diffuse large B-cell lymphomas and two *H. pylori*-negative gastric diffuse large B-cell lymphomas, and cluster II with seven *H. pylori*-negative gastric diffuse large B-cell lymphomas and one *H. pylori*-positive gastric diffuse large B-cell lymphomas (8:2 *vs* 1:7, $P=0.007$).

30 mRNAs.[22,23] Two mRNAs *FUBP3* (far upstream element binding protein 3)[24] and *ZEB1* were thus identified.

ZEB1 is a well-characterized target of miR-200,[6] whereas—to our knowledge—no experimental data are available on *FUSBP3* as a target of miR-200. Inhibition of *ZEB1* by miR-200 is, therefore, a molecular mechanism that may separate *H. pylori*-positive from *H. pylori*-negative gastric diffuse large B-cell lymphomas. The mean level of *ZEB1* was reduced from 0.37 in *H. pylori*-negative to 0.26 in *H. pylori*-positive gastric diffuse large B-cell lymphomas, $P=0.025$ (Table 3; Figure 1b).

Figure 1c further demonstrates a significant inverse correlation between *ZEB1* and miR-200 a, b, or c, with a correlation coefficient at -0.60 at $P=0.008$, -0.71 at $P<0.001$, and -0.63 at $P=0.005$, respectively.

Inhibition of *ZEB1* by miR-200 Distinguishes *H. pylori*-Positive from *H. pylori*-Negative Gastric Diffuse Large B-cell Lymphomas

Using the miR.org program, we found that miR-200 inhibits *ZEB1* and *FUBP3,* and miR-544 inhibits *CYFIP2*. No other interactions between the eight miRNAs and 30 mRNAs were identified. These findings further support a critical role of mIR-200 and *ZEB1* in *H. pylori*-positive gastric diffuse large B-cell lymphomas (Table 3).

We performed a hierarchical clustering, using all eight miRNAs from Table 2 and 30 mRNAs from Table 3. As shown in Figure 2a, cluster I included eight *H. pylori*-positive gastric diffuse large B-cell lymphomas, whereas cluster II included one *H. pylori*-positive and nine *H. pylori*-negative gastric diffuse large B-cell lymphomas (8:0 *vs* 1:9, $P<0.001$).

To estimate the significance of the miR-200-*ZEB1* pathway, we used only miR-200 and *ZEB1* for a hierarchical clustering. Cluster I included eight *H. pylori*-positive and two *H. pylori*-negative gastric diffuse large B-cell lymphomas, whereas cluster II included one *H. pylori*-positive and seven *H. pylori*-negative gastric diffuse large B-cell lymphomas (8:2 *vs* 1:7, $P=0.007$) (Figure 2b).

The miR-200-*ZEB1* pathway is almost as effective as the combined eight miRNAs and 30 mRNAs in distinguishing *H. pylori*-positive from *H. pylori*-negative gastric diffuse large B-cell lymphomas. Therefore, the miR-200-*ZEB1* is a critical pathway in separating *H. pylori*-positive form *H. pylori*-negative gastric diffuse large B-cell lymphomas. Of course, the roles of the other miRNAs in Table 2 and mRNAs in Table 3 remain to be explored.

Histopathology, Immunohistochemistry for *ZEB1* and *BCL6*, and qRT-PCR for miR-200 in *H. pylori*-Positive and *H. pylori*-Negative Gastric Diffuse Large B-cell Lymphomas

Owing to the small sample size used in genome-wide expression profiles, we used a second series of 30 *H. pylori*-positive and 30 *H. pylori*-negative gastric diffuse large B-cell lymphomas to confirm inhibition of *ZEB1* by miR-200 in *H. pylori*-positive gastric diffuse large B-cell lymphomas. This series is part of the clinical series of 102 cases.

Figure 3 shows that *H. pylori*-positive gastric diffuse large B-cell lymphomas are characterized by the presence of *Helicobacter* organisms, frequently surrounded by increased eosinophils, whereas *H. pylori*-negative gastric diffuse large B-cell lymphomas do not have *Helicobacter* organisms and demonstrate minimal eosinophilic clusters (40% *vs* 4%, $P=0.02$, Figure 3; Table 4).

Immunohistochemistry for *ZEB1* was performed and confirmed weaker expression of *ZEB1* in *H. pylori*-positive gastric diffuse large B-cell lymphomas (42% *vs* 25%, $P<0.001$, Figures 4a and b; Table 4). Immunohistochemistry for *BCL6* was also performed and showed stronger expression of *BCL6* in *H. pylori*-positive gastric diffuse large B-cell lymphomas (23% *vs* 33%, $P=0.002$, Figures 4a and c; Table 4). Finally, qRT-PCR for miR-200 was

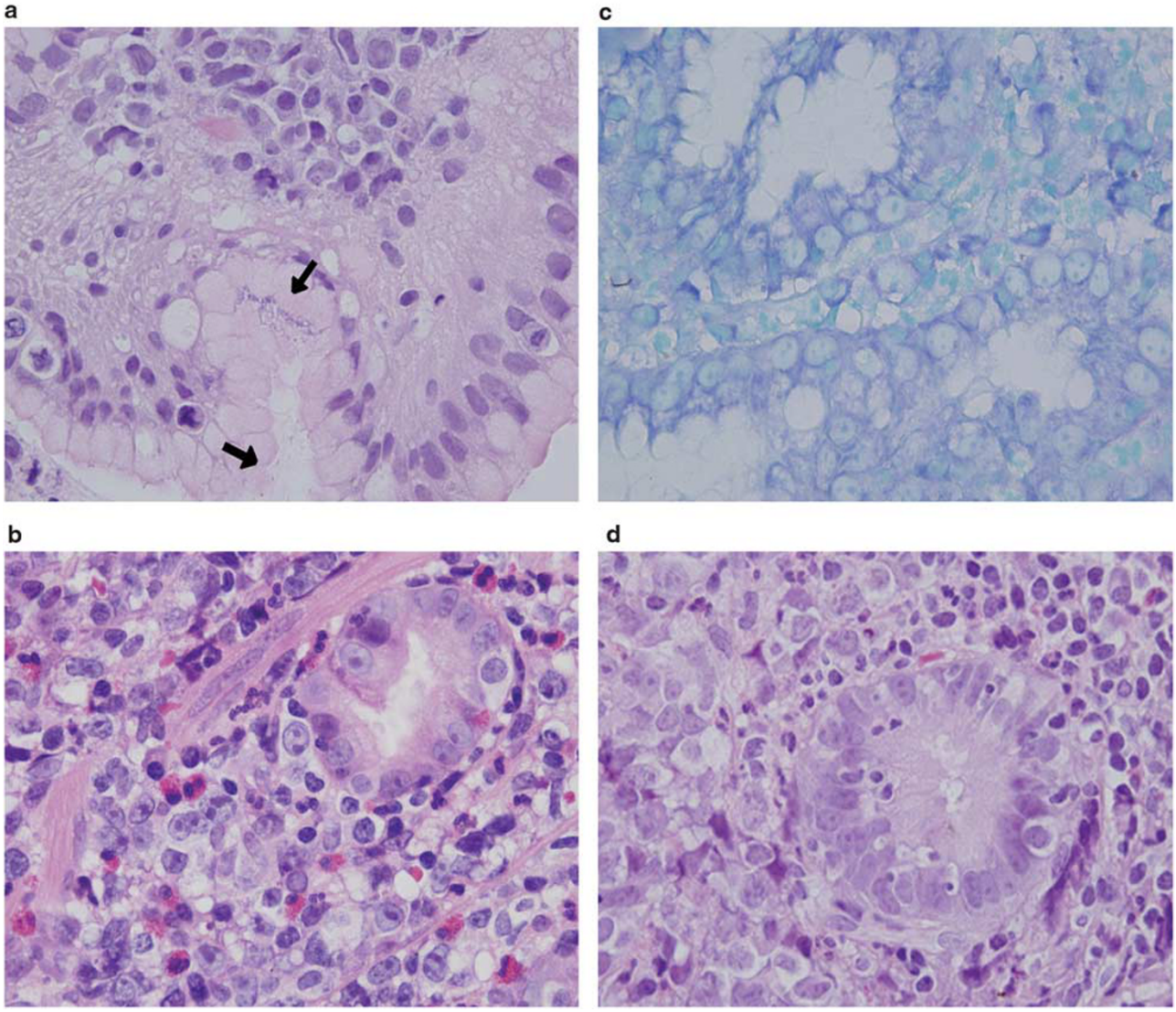

Figure 3 Histopathology of gastric diffuse large B-cell lymphomas. (**a**) Presence of *H. pylori* can be identified on H&E sections of *H. pylori*-positive gastric diffuse large B-cell lymphomas. (**b**) *H. pylori*-positive gastric diffuse large B-cell lymphomas have more inflammatory infiltrates, such as clusters of eosinophils. (**c**) *H. pylori*-negative gastric diffuse large B-cell lymphomas have no evidence of *H. pylori* even on a Diff-Quik stain. (**d**) *H. pylori*-negative gastric diffuse large B-cell lymphomas have less inflammatory infiltrates, without clusters of eosinophils. (**a, c, d**) H&E stains at $\times 1000$; (**b**) Diff-Quik stain for *H. pylori* at $\times 1000$. All stains were performed on formalin-fixed paraffin-embedded sections. An Olympus BX60 microscope with $\times 10/0.22$ ocular lens and $\times 100/1.35$ objective lens was used (Olympus, Tokyo, Japan). Arrows indicate the presence of the bacteria, *Helicobacter pylori*.

performed and confirmed higher levels of miR-200 in *H. pylori*-positive gastric diffuse large B-cell lymphomas (dC_t: 3.97 *vs* 0.26 for miR-200a at $P=0.013$, 3.64 *vs* 0.41 for miR-200b at $P=0.025$, 1.21 *vs* -1.65 for miR-200c at $P=0.018$, Figure 4d; Table 4).

As *ZEB1* suppresses *BCL6*, and *BCL6* is a known predictor of a better prognosis in gastric diffuse large B-cell lymphomas, the immunohistochemistry and qRT-PCR data are compatible with the model, in which miR-200 inhibits *ZEB1* with secondary induction of *BCL6* in *H. pylori*-positive gastric diffuse large B-cell lymphomas with a better prognosis.

Discussion

Although gastric diffuse large B-cell lymphomas are often associated with *H. pylori* infection, the biologic and clinical significance of the association is still unclear. In this study, we demonstrated that *H. pylori*-positive gastric diffuse large B-cell lymphomas have less lymph node metastasis and a better response to chemotherapy, and that this behavior could be attributed, at least partially, to a higher level of miR-200, which inhibits *ZEB1* with a secondary increase in *BCL6*.

ZEB1 is known to increase the potential for metastasis in cancers of epithelial origin through

induction of epithelial–mesenchymal transition. *ZEB1* inhibits the cell adhesion molecule E-cadherin, and, as a result of the loss of cell adhesion, increases migratory ability of the cancer cells.[5–7]

In this study, we found that expression of *ZEB1* in *H. pylori*-negative gastric diffuse large B-cell lymphomas is also associated with increased lymph node metastasis. However, in gastric diffuse large B-cell lymphomas, genome-wide mRNA expression profiles showed that the levels of E-cadherin are very low, regardless of the level of *ZEB1* (Supplementary Table S2). Therefore, *ZEB1* must have increased metastatic potential of gastric diffuse large B-cell lymphomas through another mechanism. Interestingly, loss of *BCL6* is associated with disease progression in breast cancer and gastric cancer,[25,26] suggesting that the loss of *BCL6* might be responsible for the increased lymph node metastasis in gastric diffuse large B-cell lymphomas too.

Diffuse large B-cell lymphomas of the lymph nodes can be classified into a germinal center B-cell type derived from germinal center B cells and an activated B-cell type derived from activated B cells. The germinal center B-cell type has a better prognosis than the activated B-cell type.[27] As *BCL6* is the master transcription factor for germinal center B cells,[28] the association of higher expression of *BCL6* with a better prognosis in gastric diffuse large B-cell lymphomas is consistent with the finding that nodal diffuse large B-cell lymphomas of the germinal center B-cell type have a better prognosis.[4,27] However, *BCL6* may contribute to a better prognosis through additional pathways other than promoting germinal center B-cell differentiation. The detailed molecular pathways of how *BCL6* contributes to a better prognosis remain to be clarified.

We have set a threshold for expression level at 0.1 to identify a list of 30 mRNAs differentially expressed in *H. pylori*-positive and *H. pylori*-negative gastric diffuse large B-cell lymphomas. Owing to its low expression level below the threshold of 0.1, *BCL6* is not one of the 30 mRNAs, despite

Table 4 Pathologic features of *H. pylori*-negative and *H. pylori*-positive gastric diffuse large B-cell lymphomas

	H. pylori-negative	*H. pylori*-positive	P-*value*
n	30	30	
H. pylori	0% (0/30)	100% (30/30)	<0.001
Eosinophilic cluster	13% (4/30)	40% (12/30)	0.02
Mean dC_t miR-200a	3.97	0.26	0.013
Mean dC_t miR-200b	3.64	0.41	0.025
Mean dC_t miR-200c	1.21	−1.65	0.018
ZEB1+ cells (%)[a]	42%	25%	<0.001
BCL6+ cells (%)[a]	23%	33%	0.002

[a]For each case, the percentage of *ZEB1* or *BCL6*-positive cells was determined, and the average in the *H. pylori*-positive or *H. pylori*-negative group is reported.

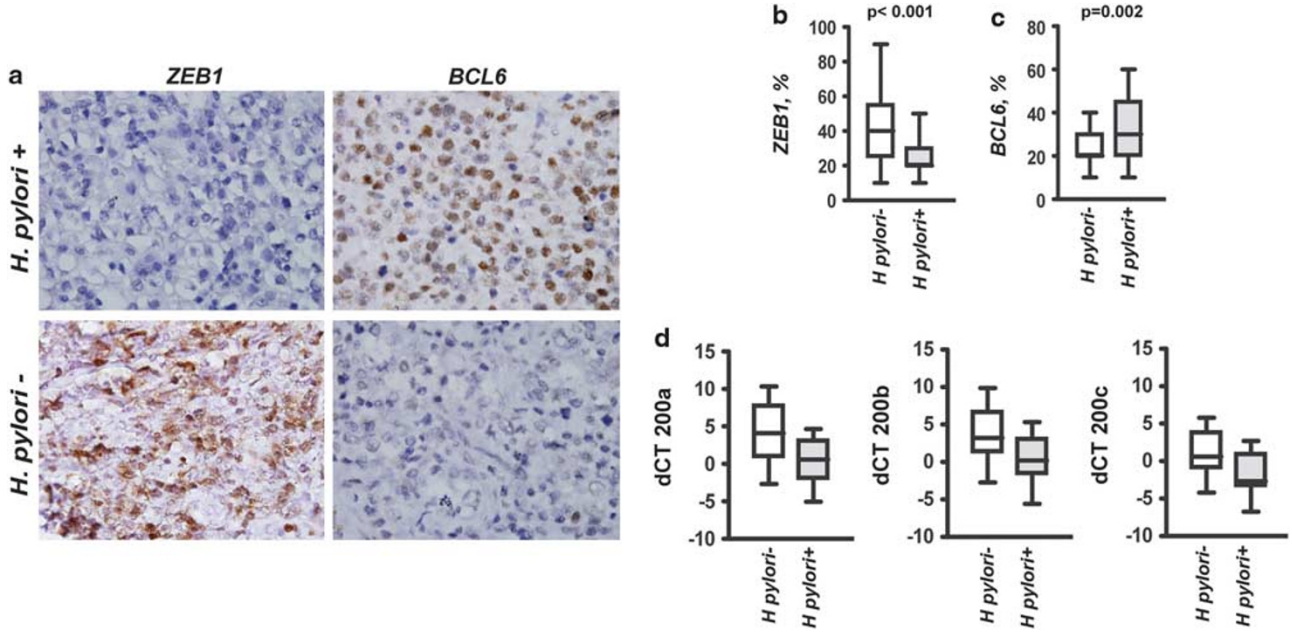

Figure 4 Immunohistochemistry for *ZEB1* and *BCL6* and qRT-PCRs for miR-200 in gastric diffuse large B-cell lymphomas. (**a**) Immunoperoxidase stains for *ZEB1* and *BCL6* in *H. pylori*-positive and *H. pylori*-negative gastric diffuse large B-cell lymphomas (×1000). An Olympus BX60 microscope with ×10/0.22 ocular lens and ×100/1.35 objective lens was used (Olympus). (**b**, **c**) Distributions for the percentages of *ZEB1*-positive (**b**) or *BCL6*-positive (**c**) cells in gastric diffuse large B-cell lymphomas. *y* axis: percentages of positive cells; *x* axis: *H. pylori*-negative *vs H. pylori*-positive gastric diffuse large B-cell lymphomas. (**d**) qRT-PCRs for miR-200 a, b, or c in gastric diffuse large B-cell lymphomas. *y* axis: dC_t; *x* axis: *H. pylori*-negative *vs H. pylori*-positive gastric diffuse large B-cell lymphomas.

its association with *H. pylori*-positive gastric diffuse large B-cell lymphomas.

H. pylori infection is also found in gastric mucosa-associated-lymphoid-tissue lymphoma, and translocation of the *H. pylori*-encoded oncoprotein cagA into the nuclei of gastric mucosa-associated-lymphoid-tissue lymphoma cells is associated with a better prognosis.[29,30] It is possible that cagA can likewise translocate into the nuclei of gastric diffuse large B-cell lymphomas to produce a better prognosis. The potential mechanisms that might have connected cagA to the activation of miR-200 remain to be clarified.

In summary, we found that *H. pylori*-positive gastric diffuse large B-cell lymphomas have less lymph node metastasis and a better response to chemotherapy, both of which could be attributed partially to the inhibition of *ZEB1* by miR-200, with secondary induction of *BCL6*. The model is consistent with previous reports on the associations between *ZEB1* and a more aggressive behavior of nodal diffuse large B-cell lymphomas[11] and between *BCL6* and a better prognosis in gastric diffuse large B-cell lymphomas.[4,31] Further studies would be needed to clarify the details of the underlying molecular mechanisms how *BCL6* reduces lymph node metastasis and/or induces sensitivity to chemotherapy. Finally, the data may be clinically important, as we have recently found that some *H. pylori*-positive gastric diffuse large B-cell lymphomas can be cured by *H. pylori* eradication therapy.[32] Further studies on the miR-200-*ZEB1*-*BCL6* pathway might identify a molecular marker that can be used to guide clinical managements of gastric diffuse large B-cell lymphomas.

Acknowledgments

The project is supported by grants NSC-102-2321-B-002-005 from the National Science Council. We are grateful for technical supports from the Tissue Bank and the bioinformatic core laboratory at the National Taiwan University Center for Genomic Medicine.

Disclosure/conflict of interest

The authors declare no conflict of interest.

References

1 Isaacson PG, Chott A, Nakamura S, *et al.* Extranodal marginal zone lymphoma of mucosa-associated lymphoid tissue (MALT lymphoma), In: Swerdlow SH, Campo E, Harris NL, *et al.* (eds). Tumours of Haematopoietic and Lymphoid Tissues, WHO Classification of Tumours. IARC Press: Lyon; 2008, pp 214–217.
2 Ferreri AJ, Montalban C. Primary diffuse large B-cell lymphoma of the stomach. Crit Rev Oncol Hematol 2007;63:65–71.
3 Psyrri A, Papageorgiou S, Economopoulos T. Primary extranodal lymphomas of stomach: clinical presentation, diagnostic pitfalls and management. Ann Oncol 2008;19:1992–1999.
4 Chen YW, Hu XT, Liang AC, *et al.* High BCL6 expression predicts better prognosis, independent of BCL6 translocation status, translocation partner, or BCL6-deregulating mutations, in gastric lymphoma. Blood 2006;108:2373–2783.
5 De Craene B, Berx G. Regulatory networks defining EMT during cancer initiation and progression. Nat Rev Cancer 2013;13:97–110.
6 Brabletz S, Brabletz T. The ZEB/miR-200 feedback loop–a motor of cellular plasticity in development and cancer? EMBO Rep 2010;11:670–677.
7 Lamouille S, Subramanyam D, Blelloch R, *et al.* Regulation of epithelial-mesenchymal and mesenchymal-epithelial transitions by microRNAs. Curr Opin Cell Biol 2013;25:200–207.
8 Papadopoulou V, Postigo A, Sánchez-Tilló E, *et al.* ZEB1 and CtBP form a repressive complex at a distal promoter element of the BCL6 locus. Biochem J 2010; 427:541–550.
9 Arnold CN, Pirie E, Dosenovic P, *et al.* A forward genetic screen reveals roles for Nfkbid, Zeb1, and Ruvbl2 in humoral immunity. Proc Natl Acad Sci USA 2012;109:12286–12293.
10 Genetta T, Ruezinsky D, Kadesch T. Displacement of an E-box-binding repressor by basic helix-loop-helix proteins: implications for B-cell specificity of the immunoglobulin heavy-chain enhancer. Mol Cell Biol 1994;14:6153–6163.
11 Lemma S, Karihtala P, Haapasaari KM, *et al.* Biological roles and prognostic values of the epithelial-mesenchymal transition-mediating transcription factors Twist, ZEB1 and Slug in diffuse large B-cell lymphoma. Histopathology 2013;62:326–333.
12 Postigo AA, Dean DC. Independent repressor domains in ZEB regulate muscle and T-cell differentiation. Mol Cell Biol 1999;19:7961–7971.
13 Brabletz T, Jung A, Hlubek F, *et al.* Negative regulation of CD4 expression in T cells by the transcriptional repressor ZEB. Int Immunol 1999;11: 1701–1708.
14 Wang J, Lee S, Teh CE, *et al.* The transcription repressor, ZEB1, cooperates with CtBP2 and HDAC1 to suppress IL-2 gene activation in T cells. Int Immunol 2009;21:227–235.
15 Nakahata S, Yamazaki S, Nakauchi H, *et al.* Downregulation of ZEB1 and overexpression of Smad7 contribute to resistance to TGF-beta1-mediated growth suppression in adult T-cell leukemia/lymphoma. Oncogene 2010;29:4157–4169.
16 Geiss GK, Bumgarner RE, Birditt B, *et al.* Direct multiplexed measurement of gene expression with color-coded probe pairs. Nat Biotechnol 2008;26: 317–325.
17 Vladislav MA. Multiplexed measurements of gene signatures in different analytes using the NanoString nCounter Assay System. BMC Research Notes 2009; 2:80.
18 Kulkarni MM. Digital multiplexed gene expression analysis using the NanoString nCounter System. Curr Protoc Mol Biol 2011; Chapter 25:Unit25B.10.
19 Sturn A, Quackenbush J, Trajanoski Z. Genesis: cluster analysis of microarray data. Bioinformatics 2002;18: 207–208.

20 Lin TC, Liu TY, Hsu SM, *et al.* The EBV-encoded miR-BART20-5p inhibits T-bet with secondary suppression of p53 in invasive nasal NK-cell lymphoma. Am J Pathol 2013;182:1865–1875.
21 Liu TY, Chen SU, Kuo SH, *et al.* E2A-positive gastric MALT lymphoma has weaker plasmacytoid infiltrates and stronger expression of the memory B-cell-associated miR-223: possible correlation with stage and treatment response. Mod Pathol 2010;23:1507–1517.
22 Betel D, Koppal A, Agius P, *et al.* MirSVR predicted target site scoring method: comprehensive modeling of microRNA targets predicts functional non-conserved and non-canonical sites. Genome Biol 2010;11:R90.
23 Betel D, Wilson M, Gabow A, *et al.* MicroRNA target predictions: the microRNA.org resource: targets and expression. Nucleic Acids Res 2008;36(Database Issue):D149–D153.
24 Chung HJ, Liu J, Dundr M, *et al.* FBPs are calibrated molecular tools to adjust gene expression. Mol Cell Biol 2006;26:6584–6597.
25 Pinto AE, André S, Silva G, *et al.* BCL-6 oncoprotein in breast cancer: loss of expression in disease progression. Pathobiology 2009;76:235–242.
26 Hirata Y, Ogasawara N, Sasaki M, *et al.* BCL6 degradation caused by the interaction with the C-terminus of pro-HB-EGF induces cyclin D2 expression in gastric cancers. Br J Cancer 2009; 100:1320–1329.
27 Barton S, Hawkes EA, Wotherspoon A, *et al.* Are we ready to stratify treatment for diffuse large B-cell lymphoma using molecular hallmarks? Oncologist 2012;17:1562–1573.
28 Basso K, Dalla-Favera R. Roles of BCL6 in normal and transformed germinal center B cells. Immunol Rev 2012;247:172–183.
29 Kuo SH, Chen LT, Lin CW, *et al.* Detection of the *Helicobacter pylori* CagA protein in gastric mucosa-associated lymphoid tissue lymphoma cells: clinical and biological significance. Blood Cancer J 2013;3:e125.
30 Lin WC, Tsai HF, Kuo SH, *et al.* Translocation of *Helicobacter pylori* CagA into human B lymphocytes, the origin of mucosa-associated lymphoid tissue lymphoma. Cancer Res 2010;70:5740–5748.
31 Chung KM, Chang ST, Huang WT, *et al.* Bcl-6 expression and lactate dehydrogenase level predict prognosis of primary gastric diffuse large B-cell lymphoma. J Formos Med Assoc 2013;112:382–389.
32 Kuo SH, Yeh KH, Wu MS, *et al. Helicobacter pylori* eradication therapy is effective in the treatment of early-stage H. pylori-positive gastric diffuse large B-cell lymphomas. Blood 2012;119:4838–4844.

Supplementary Information accompanies the paper on Modern Pathology website (http://www.nature.com/modpathol)